Available online at www.sciencedirect.com
SCIENCE DIRECT®
Catalysis Today 88 (2003) 61–72
CATALYSIS TODAY
www.elsevier.com/locate/cattod

Residence time distribution of fluids in stirred annular photoreactor

E. Sahle-Demessie [a,*], Siefu Bekele [b], U.R. Pillai [a]

[a] *National Risk Management Research Laboratory, Sustainable Technology Division, US EPA, 26 W. Martin Luther King Dr., Cincinnati, OH 45268, USA*
[b] *The Boundary Layer Wind Tunnel Laboratory, The University of Western Ontario, London, Ont., Canada*

Abstract

When gases flow through an annular photoreactor at constant rate, some of the gas spends more or less than the average residence time in the reactor. This spread of residence time can have an important effect on the performance of the reactor. This study tested how the residence time distribution (RTD) in an annular photoreactor with a magnetic stirrer at the bottom, is affected by the flow rate, different stirring rates and reactor length-to-diameter ratios. Pulse response studies with UV-Vis measurements were used to measure RTD curves, and a dimensionless parameter $L/[N(D_0 - D_i)]$ was used as a measure of the approach to plug flow.

Numerical method was used to develop a model base on second-order discritization and a convergence criteria of 10^{-4} for all variables as laminar flow. Effects of reactor mixers in an annular photoreactor were simulated using a finite volume method (Fluent). Steady state solutions were obtained by imposing boundary conditions of inlet velocity of the required flow rate, inside and outside surface of the cylinder specified a wall boundary condition and outflow boundary conditions adapted at the outlet boundary. A virtual fan having specific radial and axial flow velocities introduced at the inlet of the reactor to initiate swirl motion. Grids for the above simulations are generated using Gambit. Qualitative comparisons of the numerical results with experimental results showed that the use of axial or mixed flow stirrer could improve the flow profile narrowing the RTD curve, creating high Reynolds numbers and avoiding back mixing. The information would be useful to design and scale-up gas flow photoreactor that behave like stirred tanks in series or approach plug flow system.

Keywords: Residence time distribution; Fluids; Photoreactor; Numerical simulation

1. Introduction

In recent years, heterogeneous photocatalytic oxidation of organic compounds in the presence of a semiconductor catalyst has shown to be a promising method for the destruction of toxic chemicals in air or water [1] and for partial selective oxidation of various organic substrates [2,3]. Interest has focused on the use of TiO_2 as a photocatalyst employed in colloidal form or as an immobilized film [4,5]. In photoreactors operated with the catalyst immobilized on the outer surface, the reaction rate is predominantly determined by the light intensity on the surface, the quantum efficiency of the catalyst, the adsorption properties of the reacting components in solution, and mass transfer from the bulk of the fluid to the catalyst surface. However, little attention has been given to the use of the distribution of residence times in the analysis of performances of photoreactors.

In the real world of chemical engineering, the behavior of the reactors is often very different from that

* Corresponding author. Tel.: +1-513-569-7739; fax: +1-513-569-7677.
E-mail address: sahle-demessie.endlkachew@epa.gov (E. Sahle-Demessie).

0920-5861/$ – see front matter © 2003 Elsevier B.V. All rights reserved.
doi:10.1016/j.cattod.2003.08.009

to the ideal reactors (the perfectly mixed batch, the plug flow tubular and the perfectly mixed continuous tank reactors). The residence time distribution (RTD) of a reactor is a characteristic of the mixing that occurs in a chemical reactor. In most studies idealized plug flow or batch reactors are used, where all the flow elements in the reactor have the same residence time. Simplifying models are generally used to characterize and model non-ideal reactors the distribution of residence times in the system, and the quality of mixing [6–9]. The non-ideality of flow, which can vary with reactor size, is the uncontrolled factor in the scaling-up of reactors. The residence time distribution (RTD) of a reactor is a characteristic of the flow pattern that occurs in the chemical reactor, being one of the most informative characterization of the reactor [7,9]. The RTD gives information on how long the various elements have been in the reactor, but it does not provide any information about the exchange of matter between the fluid elements. As it provides a quantitative measure of the degree of backmixing within a system, knowledge of the liquid RTD is important for a number of reasons [9], allowing for accurate kinetic modeling of the system, and facilitating reactor design to achieve or preserve a desired flow pattern. Also, these reasons include the fact that RTD allows for a more thorough comparison between systems with different configurations or different zones of the reactor and represent a tool in successful process scale-up.

A classic annular photoreactor is considered in which a lamp is placed in the inner tube while the reaction fluid is flowing through the annulus and inside of the outer annulus is coated with the catalyst. Theoretically, it is possible to quantify deviations from ideal plug flow by measuring fluid velocities throughout the reactor to obtain a complete distribution profile [8]. A complete model of a photoreactor would require velocity vectors at each point of the system for gas phase. This information is not always available because of the complicated nature of the fluid dynamics, especially if there is an external mechanical stirrer in the reactor and because of the fact that the solution of this model needs computational efforts.

In analyzing non-ideal reactors, the RTD alone is not sufficient to determine its performance and more information is needed. To understand RTD quantitatively the experimental data have to be fitted to an adequate model (the axial dispersion model or the tank-in-series model) to describe non-ideal reactor flow pattern and know the quality of mixing especially for reactions other than those of first order. Normally fluid flow in a vertical annular reactor develops a very wide RTD, representative of parabolic velocity profile. Although static mixer placed in pipes could give flatter velocity profiles, their use may not be practical in photoreactors due to light obstruction. To have all fluid elements stay for the same time in the reactor, one needs to redistribute the fluid along the reactor length by using stirrer at the bottom of the reactor. Veeraragharan and Silverston [10] investigated the influence of vessel dimensions and fluid velocity on the RTD. The vessel length-to-diameter ratio (L/D) exerts influence on the RTD. Other studies have shown that increasing fluid flow rate decreases the width of the RTD, whereas stirring in liquid phase reactors increases the width of the RTD curve [11]. The effects of stirrer designs and stirring rates on narrowing RTD of fluids in laminar flow pipes were also studied [12].

There has been very little RTD analysis used to examine macromixing in photochemical reactors. The aim of this paper is to characterize the flow of gas phase photoreactor using the RTD analysis and numerical modeling, to determine the differences in the flow pattern in the photoreactor and improve the reactor design. We have also studied the effects of stirring on increasing mixing, narrowing the RTD curve to improve the distribution for flow elements in the reactor and reducing mass transfer limitation. These objectives were carried out in the same unit, and the obtained results could serve to choose the adequate operational configuration of the reactor.

2. Experimental

2.1. Experimental setup

The RTD of the gas phase was studied in a vertical annular reactor having a nominal volume of 2.5 l, with internal and external annular diameters of 6.8 and 9.8 cm, respectively. The length of the reactor is 56 cm, and reactor length-to-outer diameter ratio is 5.8. The reactor has annular gap of 1.5 cm and volume of 2570 cm^3. The bottom the reactor is fitted with a magnetic stirrer driven by a controlled motor connected to a tachometer (Fig. 1). The inlet gas flow rate

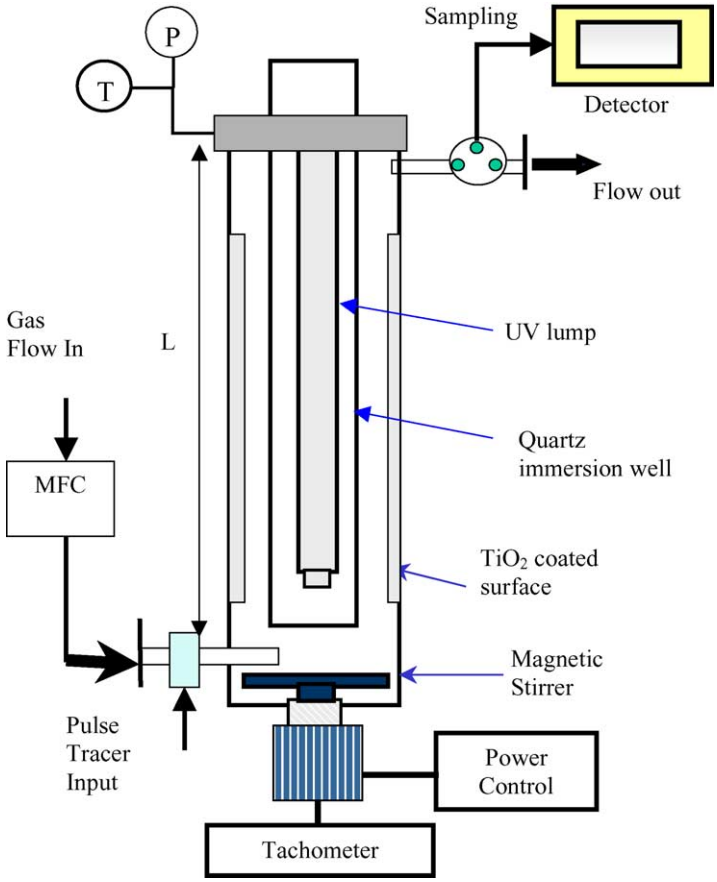

Fig. 1. Experimental setup used for the RTD study.

is controlled with a mass flow meter controller. The reactor is equipped with a stirring fan at the bottom with a power controller and a tachometer.

2.2. Measurement and modeling of RTD

The RTDs of the liquid phase were determined experimentally by using the classical tracer response technique [7]. An inert chemical tracer was injected into the reactor at a certain time ($t = 0$) and then its concentration in the effluent stream was measured as a function of time. These inputs were treated as perfect pulse inputs, although in practice it is impossible to obtain a perfect pulse; however, a rapid, turbulent injection of the tracer may approximate a perfect pulse [2,3,6]. Tracers consisting of 2 ml acetone (6.4×10^{-4} kg/m^3 reactor) were analyzed with a photo diode-array UV-Vis spectrophotometer. Tracers were injected at the entrance to the reactor to obtain the RTD curves for the reactor as a whole, and mixing entrance region. A multi-port switch valve was placed at the exit of the annular reactor for intermittent sampling of the exit flow (Fig. 1).

It was assumed that a reasonable pulse at the reactor entrance was obtained: the injection took place over a very short period compared to the residence time in the various segments of the reactor, and it was assumed that negligible amounts of dispersion have occurred between the point of injection and the entrance of the reactor system. The flow is consider to be at steady state with no adsorption. The volume of tracer used was kept small in relation to the total volume within the reactor and the injection was carried out as quickly and smoothly as possible. The effluent concentration–time

curve is referred to as the C curve in RTD analysis. We choose an increment of time (Δt) small enough so that the concentration of tracer, exiting between Δt and $t + \Delta t$ is essentially constant. The curve $C(t)$ allowed us to determine the residence time function (or the exit-age distribution function), that describes in a quantitative manner the residence time of different fluid elements within the reactor.

The first and second moments of the RTD function, known as the residence time and the variance or dispersion, respectively, were also determined. To obtain the $E(t)$ curve from the $C(t)$ curve, we just divided $C(t)$ by the integral

$$\int_0^\infty C(t)\,\mathrm{d}(t) \tag{1}$$

which is the area under the C curve. This area can be found using the graphical integration

$$E(t_i) = \frac{C(t)}{\sum_{i=1}^{n} C(t_i)\,\Delta t_i} \tag{2}$$

$E(t)$ is the most frequently used of the distribution functions which are related to reactor analysis.

The performances of the non-ideal reactors was analyzed using the RTD data either directly, as in the precedent paragraph or in relation with flow models. To characterize quantitatively the RTD in annular reactor the single parameter model, tank-in-series model was chosen. The tanks-in-series model, where the real annular reactor is replaced by a series of consecutive, equal volume ideally stirred tank reactors, N, resulting in the same longitudinal mixing effect. For a given vessel, the higher the number of tanks in series the closer one approaches plugs flow. In the present study the effectiveness of flow rates, various designs of stirrer and stirring rates was tested to determine which would give the closest approach to plug flow.

The responses to a pulse input of tracer gives the RTD curve directly. Comparing the experimental RTD curve with a family of curves for the tanks-in-series model represents the simplest stage-wise model for non-ideal flow. The curve C for N tank-in-series can be expressed by [7]:

$$\bar{t}E_t = \left(\frac{t}{\bar{t}}\right)^{N-1} \frac{N^N\,\mathrm{e}^{-tN/t}}{(N-1)!} \tag{3}$$

where the functions of distribution were obtained as discrete values of the concentration at the time (that is $C(\Delta t_i)$), the values of the residence time and the variance were obtained from the following relationships:

$$\bar{t} \cong \frac{\sum t_i C(t_i)\,\Delta t_i}{\sum C(t_i)\,\Delta t} \tag{4}$$

$$\sigma^2 \cong \frac{\sum (t_i - \bar{t}) C(t_i)\,\Delta t_i}{\sum C(t_i)\,\Delta t_i} \tag{5}$$

Levenspiel [13] suggested ways of finding the values of N from experimental RTD curves. The variance of curves expressed as

$$N = \frac{\bar{t}^2}{\sigma^2} \tag{6}$$

where σ^2 is the variance of the RTD curve calculated from the experimental response curve as shown in Eq. (3). For a given reactor length L and annular diameters D_0 and D_i a dimensionless group

$$\frac{L}{N(D_0 - D_i)} \tag{7}$$

can be defined which represents the length of the reactor in terms of annular space that is equivalent to a stirred tank. The aim of this study was to find the type of flow conditions and mixing speed which would minimize $L/[N(D_0 - D_i)]$, since this presents the narrowest RTD and closest approach to plug flow.

The normalized RTD were also used by defining the dimensionless time in the following form [7]:

$$\theta = \frac{\text{actual time}}{\text{mean residence time}} = \frac{t}{\bar{t}}$$

The dimensionless function was defined as

$$E(\theta) = \bar{t}E(t) \tag{8}$$

$$\int_0^\infty E(\theta)\,\mathrm{d}\theta = 1 \tag{9}$$

Also, the internal age distribution was analyzed. This is the fraction of material inside the reactor characterizing the time the material has been (and still is in) the reactor at a particular time. This distribution is in a close analogy to the external age distribution. The relation between the internal age distribution and $E(\theta)$ is in the following form:

$$I(\theta) = 1 - \int_0^\infty E(\theta)\,\mathrm{d}(\theta) \tag{10}$$

$I(\theta)$ supplies information on the particular state of a reactor mixture. The intensity function $\lambda(\theta)$, also is

a measure of flow deficiencies and is determined as follows:

$$\lambda(\theta) = \frac{E(\theta)}{I(\theta)} \tag{11}$$

2.3. Experimental method

The annular reactor was operated in a continuous flow of air at 60 °C. The inflow volumetric gas flow rate Q_1, the superficial velocity in the reactor u, and the fan speed were chosen as independent variables. The RTD distribution functions were obtained from the experimental $C_i - t_i$ values. Together with the mean distribution time and the dispersion values two operational parameters, airflow rates and fan speeds, were studied.

Most photoreactor design studies are focused on the distribution and usage of light and assumed flow patterns are ideal. The aim of this paper is to improve residence time distribution of flow elements in photoreactors, increasing the Reynolds number and turbulence for the flow, and enhance contact of the fluid with immobilized catalyst. This helps to achieve better control of the reactor performance. Therefore, it is necessary to perform a comparative study by using a stirring fan and optimizing the required speed.

3. Results and discussion

3.1. Characteristics and profiles of RTD functions

Totally 16 experiments were carried out in two replicates at 60 °C, by which two process parameters were varied. Four gas velocities and four agitation rates were measured. The superficial gas velocity was estimated in the range of 4.2×10^{-4} to 2.7×10^{-3} m/s, and impeller agitation rates were varied from 100 to 960 rpm.

The normalized functions were used in order to compare the flow patterns inside the reactor at four levels of flow rates and three levels of fan speed. The response curves to a Dirac impulse were plotted for every experimental point in the two operational modes presented above, allowing for the determination of the age distribution functions [$E(\theta)$, $I(\theta)$, $\lambda(\theta)$], as well as the first and second moments of the RTD.

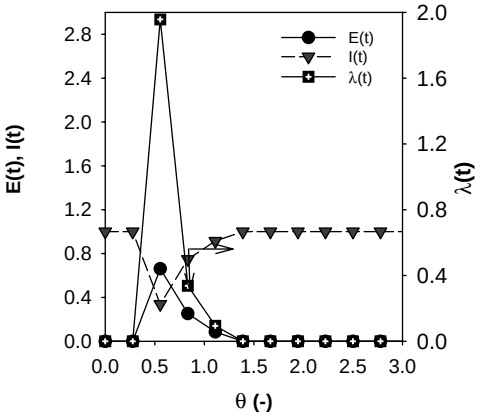

Fig. 2. The RTD functions in the annular reactor for flow rate of 1 l/min and without stirring fan.

The typical RTD data showed that there is a short delay during which little or no tracer was detected at the exit of the reactor. This was accompanied by a sharp rise in tracer concentration followed by a steady decrease. The flow behavior in the overall reactor indicates a great deviation from the ideal plug flow model. In Fig. 2, the experimental $C_i - t_i$ curves were used to obtain information about, the mean fluid residence time, the variance of distributions, σ^2; the RTD distribution functions at the reactor exit, inclusively in normalized form, $E(\theta)$, the distribution ages inside the reactor, $I(\theta)$, and the intensity of distribution, $\lambda(\theta)$. They were found to be dependent on the fluid flow rate, Q_1, and superficial velocity. The RTD functions generally characterize a non-ideal flow, which significantly deviates from the ideal plug flow.

Fig. 3 shows the $E(\theta)$ versus θ curves for the reactor without stirring at different flow rates. It can be seen that the RTD curve narrows with increasing flow rates. The curves, $E(\theta)$ shows the presence of stagnant zones and channeling. Also, the maximum of the curve $E(\theta)$ which appears at $\theta < 1$ indicates the presence of the short-circuits. The effects of flow rate on parameter $L/[N(D_0 - D_i)]$ and mean residence time is shown in Fig. 4. As the flow rate increased from 1 to 6.5 l/min the measured mean residence time decreased proportionally. The estimated Reynolds number indicated laminar flow. As the flow rate increased from 1 l/min, where the flow showed to be far from ideal plug flow conditions, to 3.5 l/min, the parameter $L/[N(D_0 - D_i)]$ value decreased sharply. However,

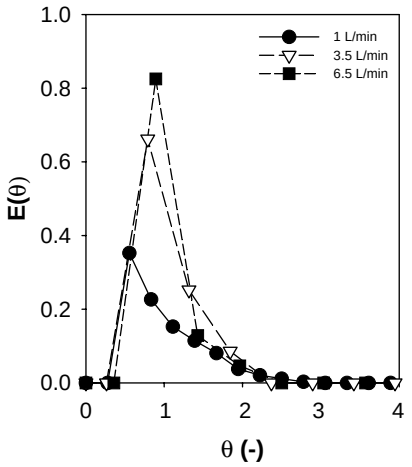

Fig. 3. Typical RTD curves at different flow rates.

further increase in flow rate decreased the RTD function at a lower rate.

Fig. 5(a) and (b) displays the effect of increased stirring on the RTD curves at 2 and 6.5 l/min, respectively. It can be seen that although slow stirring could increase mixing and narrow the RTD curve, increasing rpm widens the RTD curve. Fig. 6 shows the effects of both air flow rate and agitation speed on the parameter $L/[N(D_0 - D_i)]$, where the optimum rpm is somewhere 150–200 rpm.

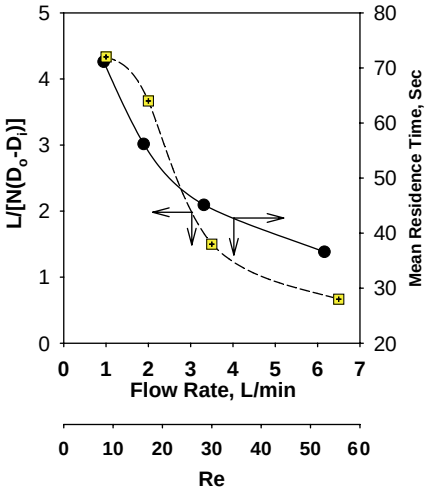

Fig. 4. The effects of flow rate on the value of $L/N(D_0 - D_i)$.

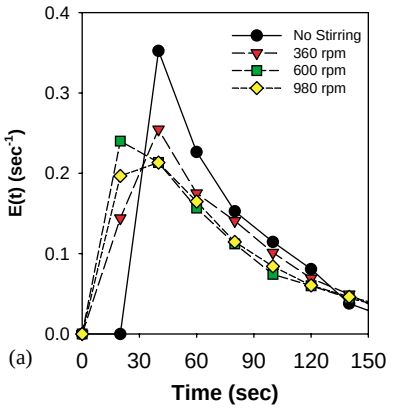

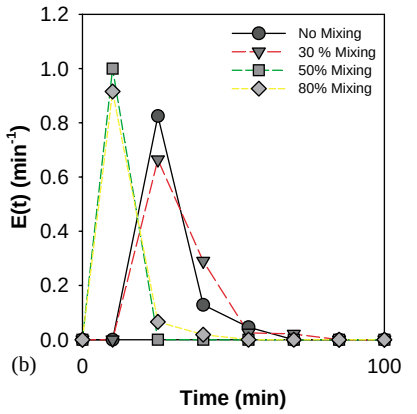

Fig. 5. Typical RTD curves at different stirrer rpms at inlet flow rates: (a) 1 and (b) 6.5 l/min.

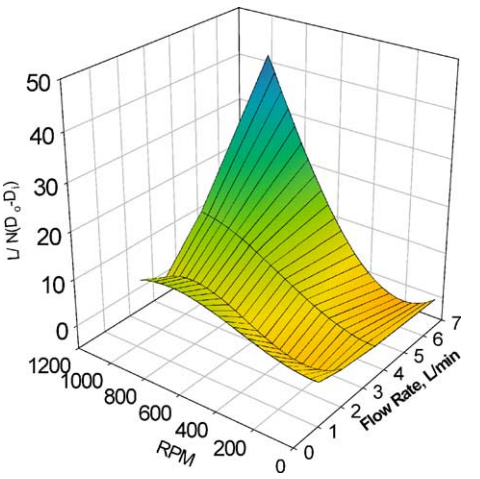

Fig. 6. Three-dimensional dimensional variation of $L/[N(D_0-D_i)]$ with flow rates and stirrer rpm.

4. Numerical setup

4.1. Domain and mesh specifications

The computational domains were generated for pipes with inner diameter of 6 cm and external diameters of 8, 10, 12, 14 cm and length of 1.2 and 2.4 m. The mesh size of 10 cells in radial, 120 cells in axial are used. Along the length, 300 cells for the 1.2 m and 600 cells for 2.4 m length are employed. Thus the cell sizes of 360,000 and 720,000 were used for simulation of 1.2 and 2.4 m long, respectively. Structural meshes were used to take the advantage of flow directionality for increasing the convergence rate and also to minimize error in computational approximation [14]. The meshes were generated using Gambit [15], Fig. 7. Once the flow fields were fairly defined, known number of particles were released to simulate tracer injection. The released particles were tracked using the discritized control volume aspect ratio in the general computational domain.

4.2. Boundary condition

The numerical investigations were done for two categories; mainly flow without fan and with fan. For the flow simulation without fan, axial velocity ranged from 1.66×10^{-3} to 3.3×10^{-3} m/s, which corresponds 0.5–10 l/m flow rate, respectively. Three types of fans, axial, mixed and radial were simulated. These fans were virtual fans where the axial, angular and radial velocities were specified at 1 cm from the inlet to achieve the desired swirl motion. The prescribed fan velocities depended on the blade angle, hub diameter and fan angular speed. The relation between the components of fan velocities, blade angle hub diameter is given by Eq. (12) [16]:

$$V_{u_2} = U_2 - V_x \cot(b_2), \quad U_2 = rN \tag{12}$$

where r is the radius of hub, N the angular speed in rpm, b_2 the exit angle of fan blade, V_x the axial velocity of the incoming fluid and V_{u_2} the radial velocity. A fan speed of 200 rpm is used for the simulation.

The inner and outer surfaces of the pipe were specified as no slip boundary condition employed. The outflow boundary condition at the outlet adapted the values at the outlet interpolated from the interior domain.

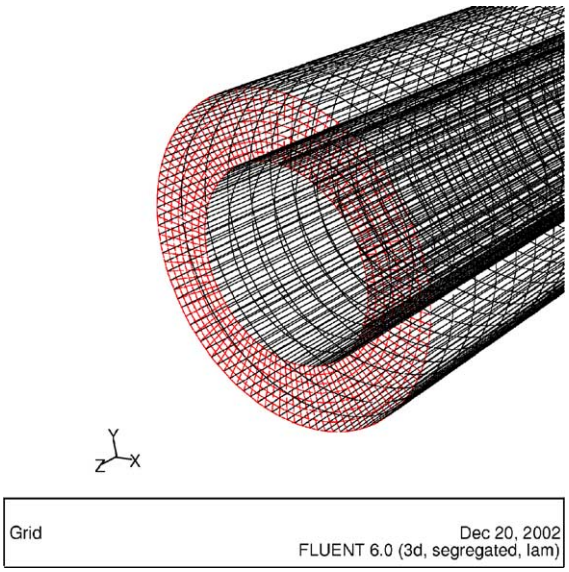

Fig. 7. Mesh grid used for the numerical simulation for the annular reactor.

4.3. Mathematical formulation

The equation for laminar incompressible fluid flowing stead state in a vertical annular region with an agitator at the bottom is solved numerically. We begin by setting up mass conservation equation for incompressible flow [17]:

$$\frac{\partial(\rho u_i)}{\partial x_i} = 0 \tag{13}$$

The momentum balance over a thin cylindrical shell can be determined using the following equation:

$$\frac{\partial(\rho u_j u_i)}{\partial x_j} = -\frac{\partial P}{\partial x_i} + \frac{\partial}{\partial x_j}\left[\mu\left(\frac{\partial u_i}{\partial x_j} + \frac{\partial u_j}{\partial x_i}\right)\right] \tag{14}$$

where P is the static pressure, μ the dynamic viscosity, ρ the fluid density and u_i are components of fluid velocity.

The above equations were descrtized using second-order scheme. Fluent 5 [18] is used for all numerical simulations. A convergence criterion of 10^{-4} is specified for all computations before any result is admitted as a solution.

Once convergence of steady state flow was established, residence time computations were preformed by solving the transport equation of motion based on

a known flow field particle tracking, given by the following equation:

$$\frac{du_p}{dt} = F_D(u - u_p) + \frac{g_x(\rho_p - \rho)}{\rho_p} \quad (15)$$

where F_D $(u - u_p)$ is the drag force per unit particle mass, u the fluid velocity, u_p the particle velocity, r_p the density of particle, g_x the force of gravity and F_D is given by the following relations:

$$F_D = \frac{18\mu C_D Re}{24\rho_p d_p^2} \quad (16)$$

where C_D is the drag coefficient, Re the relative Reynolds number, d_p the particle diameter. Drag coefficient and Reynolds number are given by the

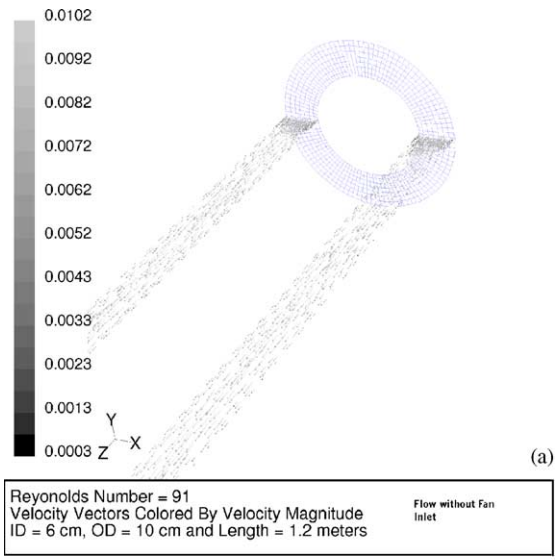

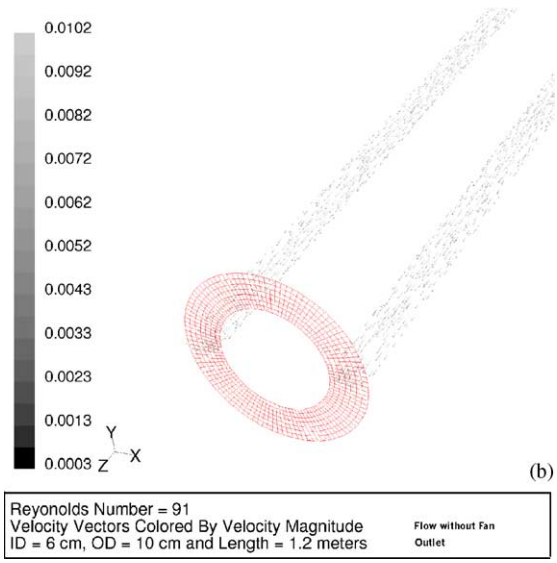

Fig. 8. Velocity vector at the (a) inlet and (b) outlet of continuous flow annular reactor for the case without stirring fan.

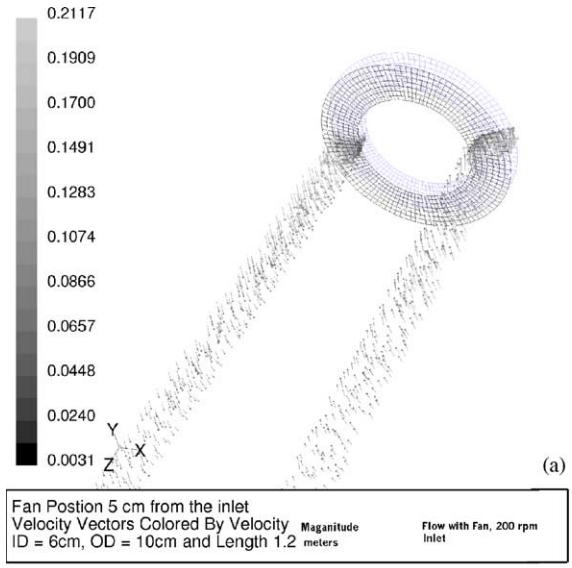

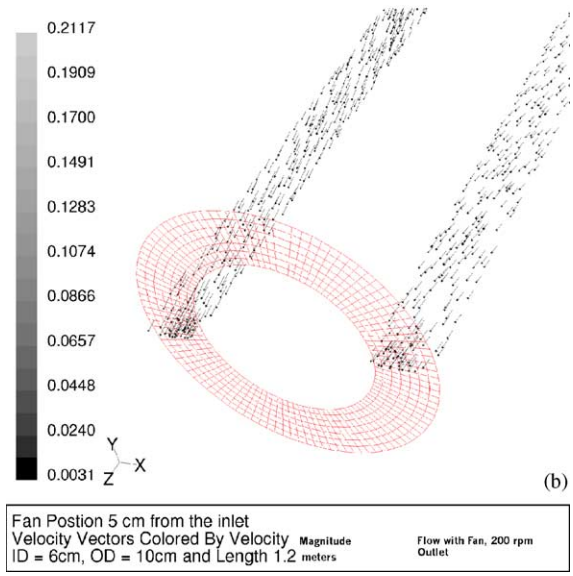

Fig. 9. Velocity vector at the (a) inlet and (b) outlet of continuous flow annular reactor with stirring fan.

equations

$$C_D = a_1 + \frac{a_2}{Re} + \frac{a_3}{Re^2} \quad (17)$$

and

$$Re = \frac{\rho d_p (u_p - u)}{\mu} \quad (18)$$

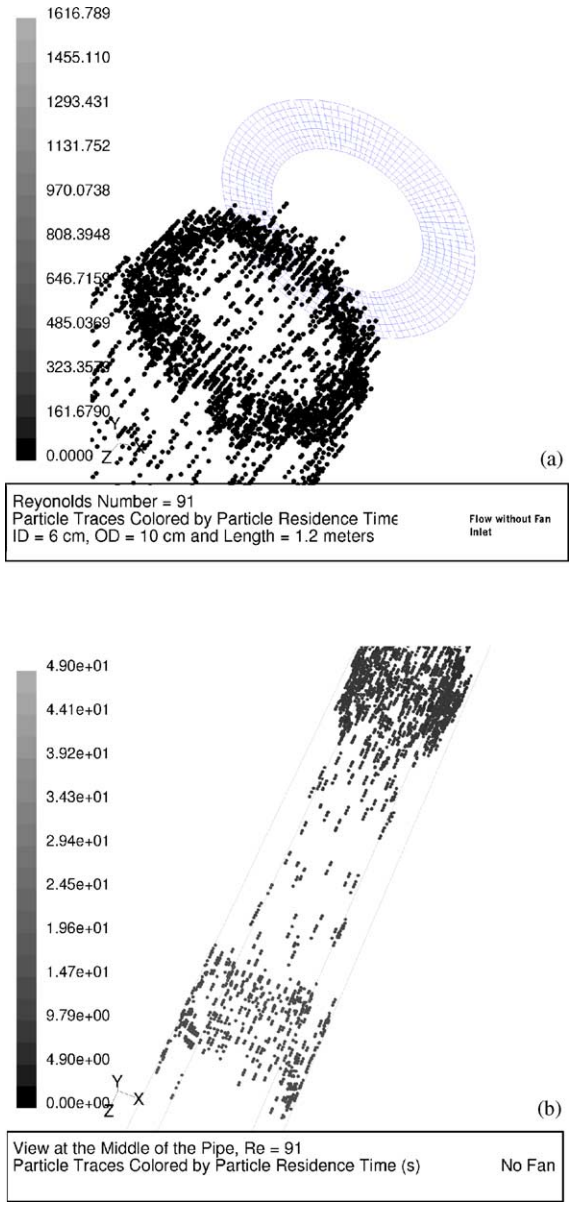

Fig. 10. Particle distributions at the (a) inlet and (b) middle of continuous flow annular reactor without stirring fan.

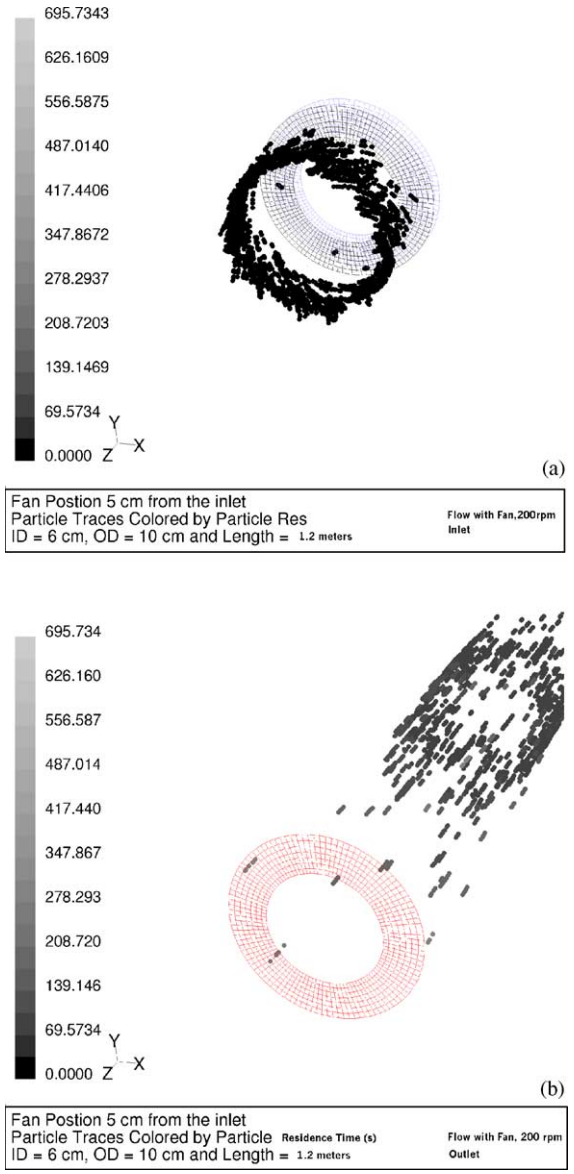

Fig. 11. Particle distributions at the (a) inlet and (b) outlet of continuous flow annular reactor with stirring fan.

a_1, a_2 a_3 are constants that apply over several ranges of Reynolds number given by Morris and Alexander [16].

Eq. (15) solved for particles released from inlet surface. A total of 900 time steps specified for measuring the residence time and for visualization of the flow pattern for all cases. Each step has a duration of 1 s. The number of total steps selected is based on repeated

Table 1
Results of numerical simulation of particles residence time

Case number	Diameter		Length (cm)	Flow rate (l/min)	Fan	Type of fan	Speed (rpm)	Number of particles released	Number of particles incomplete	Number of particles escaped	Elapsed time min (s)	Elapsed time maximum (s)	Elapsed time mean (s)	Elapsed time standard deviation (s)
	External (cm)	Internal (cm)												
1	10	6	120	2	No	–	–	742	62	680	131	1075	205	117
2	10	6	120	0.5	No	–	–	742	56	686	506	2425	786	377
3	10	6	120	6	No	–	–	742	96	646	45	456	78	65
4	10	6	120	2	Yes	Axial	200	742	25	717	129	594	141	40
5	10	6	120	2	Yes	Radial	200	742	712	31	7	33	27	7
6	10	6	120	2	Yes	Mixed	200	742	30	712	129	696	141	41
7	8	6	120	2	No	–	–	408	262	146	62	464	125	87
8	8	6	120	0.875	No	–	–	408	204	204	140	1122	332	22
9	12	6	120	2	No	–	–	456	9	447	212	1627	327	185
10	12	6	120	3.375	No	–	–	456	13	443	127	827	193	110
11	14	6	120	2	No	–	–	704	17	684	312	1449	465	251
12	14	6	120	4	No	–	–	704	17	687	158	748	231	121
13	10	6	240	2	No	–	–	742	190	552	55	299	66	21

observations of the particle motion, which showed that 900 steps are sufficient enough to obtain statistical values. In the computation of particle tracking, the particles are reported as escaped or incomplete within the specified length of time.

4.4. Numerical result

The steady state flow field of two cases, without and with fan, their velocity vectors are given in Figs. 8 and 9. For clarity, only section of the pipe at the inlet and outlet of the flow are plotted. Fig. 8(a) and (b) shows the case of flow without fan at the inlet and outlet of the flow, respectively. It can be observed that the flow is purely axial at the inlet as well as at the outlet. Fig. 9(a) and (b) shows the case with fan at the inlet and outlet of the flow, respectively. The swirl motion produced by the fan can be seen at the inlet plot of Fig. 9(a). This influence is carried down and can be seen at the outlet plot, Fig. 9(b). The above cases have inner diameter of 6 cm, outer diameter of 10 cm and length of 1.2 m.

The particle trajectory computation delivers the distribution of the particles and how closely packed they are at the beginning as well as how far they are transported. Fig. 10(a) and (b) shows the particle distribution at the inlet and the outlet for the case without fan. Fig. 11(a) and (b) shows the particle distribution in the case of flow with the presence of the fan. Comparing Fig. 10(a) and (b) with Fig. 11(a) and (b), one can easily observe the effect of the fan, which narrows the spread of the donut shaped particle distribution in the annular space.

The residence time of particles with change in the flow rate, length and with and without fan are given in Table 1. The elapse time of the particles released agreed well with experimental RTD observation. With the increase in flow rate with no stirring fan, the mean residence times and their variances of the flow elements in the annular decreased proportionally. However, without a stirring fan 7–12% of the particles did not completely leave the reactor after a period of six times the mean residence time, indicating the presence of back mixing. For a constant flow rate of 2 l/min in annular reactor of outer and inner diameters of 10 and 6 cm, the use of an axial or mixed flow fan reduced the mean residence time by about 30% while eliminating all back flows. However, radial flow fan creates high amount of back mixing where 95% of particles do not leave the reactor. The effect of the annular gap width on the RTD of flow elements was also investigated. The results are reported in Table 1. For the case with no stirring fan, increasing the length of the annular reactor (case 13) allowed to narrow the RTD curve. For the annular reactor with no stirring effect, wider annular gap increases the variance, and reduces back mixing. Therefore, qualitative comparisons of the numerical results with experimental results showed that the use of an axial or mixed flow stirrer could improve the flow profile by narrowing the RTD curve, creating high Reynolds numbers, and avoiding back mixing.

5. Conclusions

Data on the RTD of fluid particles in the exit stream of an annular flow reactor were obtained using the classical pulse-response technique. They were used to investigate some aspects of flow behavior of the photoreactor. The data were also used for gas phase flow diagnosis in the reactor with and without stirrer. These concluding remarks were confirmed by the experimental profiles of the distribution functions of internal ages $I(\theta)$, as well as by the intensity distribution function $l(\theta)$. The RTD functions demonstrated significant deviation from plug flow condition, where the mean residence time was much lower than the space–time. The dimensionless quantity $L/[N(D_0 - D_i)]$ is the appropriate measure of the narrowing the RTD curve to determine the approach to plug flow conditions. This study showed that a stirrer at the optimum rpm placed at the bottom of an annular reactor, could help narrow the RTD curve, and could improve mass transfer for surface reactions. The optimum rpm was in the range from 150 to 250. At the optimum rpm the length of the reactor that is double of the annular gap, $2(D_0 - D_i)$, behaved as one ideal stirred tank. Higher stirring rate broadened the RTD curve drastically, where the reactor increasingly behaved as a single stirred tank reactor. Numerical simulation helped us to investigate the effects of stirring, fan type, and annular gap space on the mean and variance of elapsed time of flow elements and the possibility of back mixing. Qualitative comparisons of the numerical results with experimental results show that the use of axial or mixed flow

stirrers could improve the flow profile narrowing by the RTD curve, creating high Reynolds numbers, and avoiding back mixing.

References

[1] D.F. Ollis, E. Pelizzetti, N. Serpone, Photocatalysis: Fundamentals and Applications, Wiley, New York, 1989.
[2] A. Maldotti, A. Molinari, R. Amadelli, Chem. Rev. 102 (2002) 3811–3826.
[3] U.R. Pillai, E. Sahle-Demessie, J. Catal. 211 (2) (2002) 434–444.
[4] O. Legrini, E. Oliveros, A.M. Braun, Chem. Rev. 93 (1993) 671.
[5] M.R. Hoffmann, S.C. Martin, W. Choi, D.W. Bahbemann, Chem. Rev. 95 (1995) 69.
[6] H. Blenke, in: T.K. Ghose, A. Fiechter, N. Blackebrough (Eds.), Advances in Biochemical Engineering, vol. 13, Springer, Berlin, 1979, pp. 120–214.
[7] O. Levenspiel, Chemical Reaction Engineering, Wiley, New York, 1972.
[8] D.E. Swaine, A.J. Daugulis, Review of liquid mixing in packed bed biological reactors, Biotech. Progr. 4 (1988) 134–148.
[9] S.H. Fogler, Elements of Chemical Reaction Engineering, Prentice-Hall International, New Jersey, 1992.
[10] S. Veeraragharan, L. Silverston, Can. J. Chem. Eng. 19 (1971) 346.
[11] K.H. Reichert, H.U. Moritz, J. Appl. Polym. Sci.: Appl. Polym. Symp. 36 (1981) 151–164.
[12] G.T. Zhang, N. Wannenmacher, A. Haider, O. Levenspiel, Chem. Eng. J. 45 (1990) 43–48.
[13] O. Levenspiel, The Chemical Reactor Omnibook, OSU Bookstore, Corvallis, OR, 1989.
[14] J.H. Ferzinger, Peric, Computational Method in Fluid Dynamics, Springer, New York, 1999.
[15] Gambit, User Guide, Fluent, 1998.
[16] S.A. Morris, A.J. Alexander, An investigation of particle trajectories in two-phase flow systems, J. Fluid Mech. 55 (2) (1972) 193–208.
[17] R.B. Bird, W.E. Stewart, E.N. Lightfoot, Transport Phenomena, Wiley, New York, 1960.
[18] Fluent, User Guide, Fluent, 1998.